Extended version of a contribution to the 16th World Conference on Nondestructive Testing, Montréal, Canada, August 30 - September 3, 2004

DETECTION AND CHARACTERIZATION OF FERROMAGNETIC INCLUSIONS IN NON-FERROMAGNETIC ALLOYS

J. H. Hinken[1)], H. Wrobel[1)], G. Mook[2)] and J. Simonin [2)]

[1)] University of Applied Science, Magdeburg, Germany

[2)] University of Magdeburg, Magdeburg, Germany

Abstract

Ferromagnetic inclusions can origin from splintering or breaking of tools. Without changing the surface geometry they occur as defects close to the surface. If they lead to a potential risk they have to be detected and characterized. For this purpose two complementary NDT methods have been developed. The magnetometry allows a most sensitive detection of the inclusions while the multi-frequency eddy current technique allows for more detailed information regarding the position and the shape of the particle.
At first this paper presents a recently developed fluxgate-gradiometer of second order. This allows to detect previously magnetized particles with a mass down to a few milligram from distances up to 100 millimeter. Also first statements on the particle orientation are possible. The gradiometer arrangement suppresses the magnetic noise of the environment. Compared to superconducting SQUID-magnetometers, the residual noise is of the same order; however the fluxgate version can be handled much easier because no cooling is necessary for operation.
While the magnetometry makes use of the magnetic remanence of the inclusion, the multi-frequency eddy current technique uses the difference in the magnetic permeability between particle and the matrix material. An analysis of the signal caused by local permeability changes is given. Furthermore suitable sensors are presented as well as strategies for signal evaluation, signal interpretation and visualisation.

1. Introduction

In many technical situations ferromagnetic inclusions in a non-ferromagnetic surrounding cause problems. A few examples are given in the following. Extremely small iron particles in turbine discs are dangerous and have to be detected before using the discs [1], [2]. Also the housing of superconducting particle accelerators, which is normally made from niobium, must not contain any ferromagnetic particles to avoid quenching. And during recycling of light metals as aluminium or magnesium the components have to be checked for ferromagnetic inclusions, also. Ferromagnetic regions within a non-ferromagnetic surrounding also occur during fatigue of stainless steel which leads to the generation of delta ferrite. Also in non-ferromagnetic alloys which consist of ferromagnetic components, e.g. Nickel based alloys, ferromagnetic regions can occur after too extensive heating of the surface or even recasting of a surface layer. Furthermore during a manufacturing process tools can splinter or break and leave extremely small particles in the work piece; these can be of ferromagnetic nature and in critical components they have to be detected and assessed with respect to their size and dangerousness.
This paper will concentrate on the detection of ferromagnetic particles caused by splintering or

breaking of tools. For the detection of such ferromagnetic inclusions two methods can be used. They can be explained using figure 1.

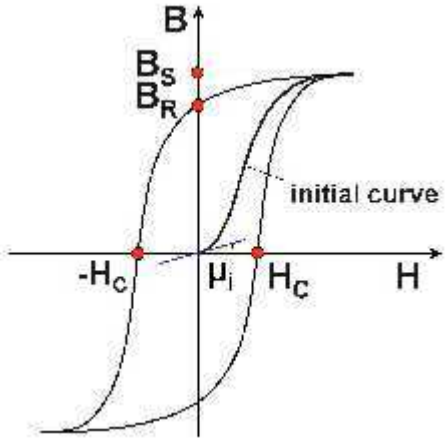

Figure 1: Principal magnetisation curve of ferromagnetic material: H- magnetic field strength, B- magnetic flux density

The first method makes use of the magnetic remanence BR of the particles. Using this magnetic remanence method (MRM), in a first phase the device under test is brought into a strong dc magnetic field. If ferromagnetic particles are present they are magnetised near to saturation magnetisation BS. In phase two the magnetic field which acts on the device under test is made zero and the ferromagnetic inclusions, if present, act as small permanent magnets with remanent magnetisation BR. Then the surface of the device under test is scanned by a most sensitive magnetometer. Magnetic field signatures then indicate a ferromagnetic inclusion whose size and depth below the surface can be estimated [1], [2].
The second method to detect ferromagnetic inclusions is the eddy current (EC) technique responding to the difference in the magnetic permeability and the conductivity between the particle and the matrix material. The overwhelming influence is expected by the permeability effect. The magnetic permeability of the particle is the initial permeability µi shown in figure 1 and that of the non-ferromagnetic matrix is µ0. For the analysis of the signal a multi-frequency technique is advantageous. In the eddy current xy-plots the phase can be tuned such that a deviation in x-direction responds to the lift-off and a change in y-direction mostly responds to a change in permeability.

2. Results

Samples with natural and artificial ferromagnetic inclusions have been tested by using the MRM method and the EC testing.
In phase one of the MRM method the samples had been premagnetized in a magnetic flux density of about 0.3T, realised by a strong permanent magnet. The measurement setup is described in [3]. The magnetic sensors are fluxgates of type Bartington MAG-03IEL100. They are arranged in a gradiometer setup and the samples can be rotated under the sensors according to figure 2.

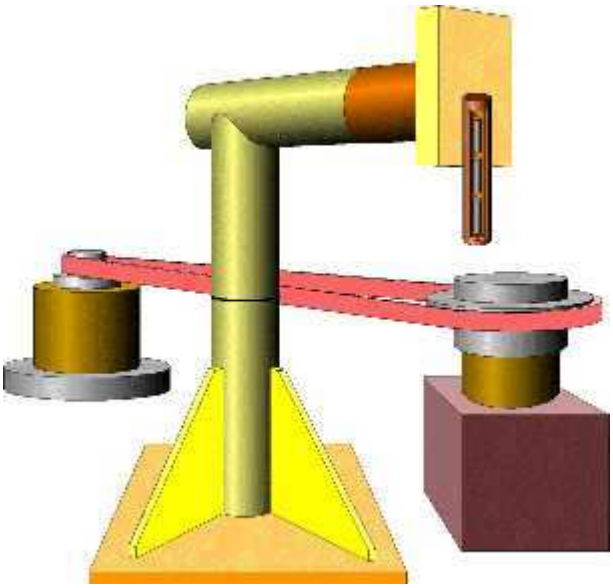

Figure 2: Principal View of Fluxgate Gradiometer

The gradiometer setup is necessary to exclude the extremely strong background fields, e.g. earth magnetic field and ac magnetic fields, stemming from power lines. With a magnetic field gradiometer it is possible to measure extremely small magnetic fields stemming from nearby sources while strong homogeneous background fields are present. Figure 3 shows the noise spectrum of the used gradiometer of second order which consists of three coaxially in line placed magnetic sensors. These three sensors can be seen in figure 2.

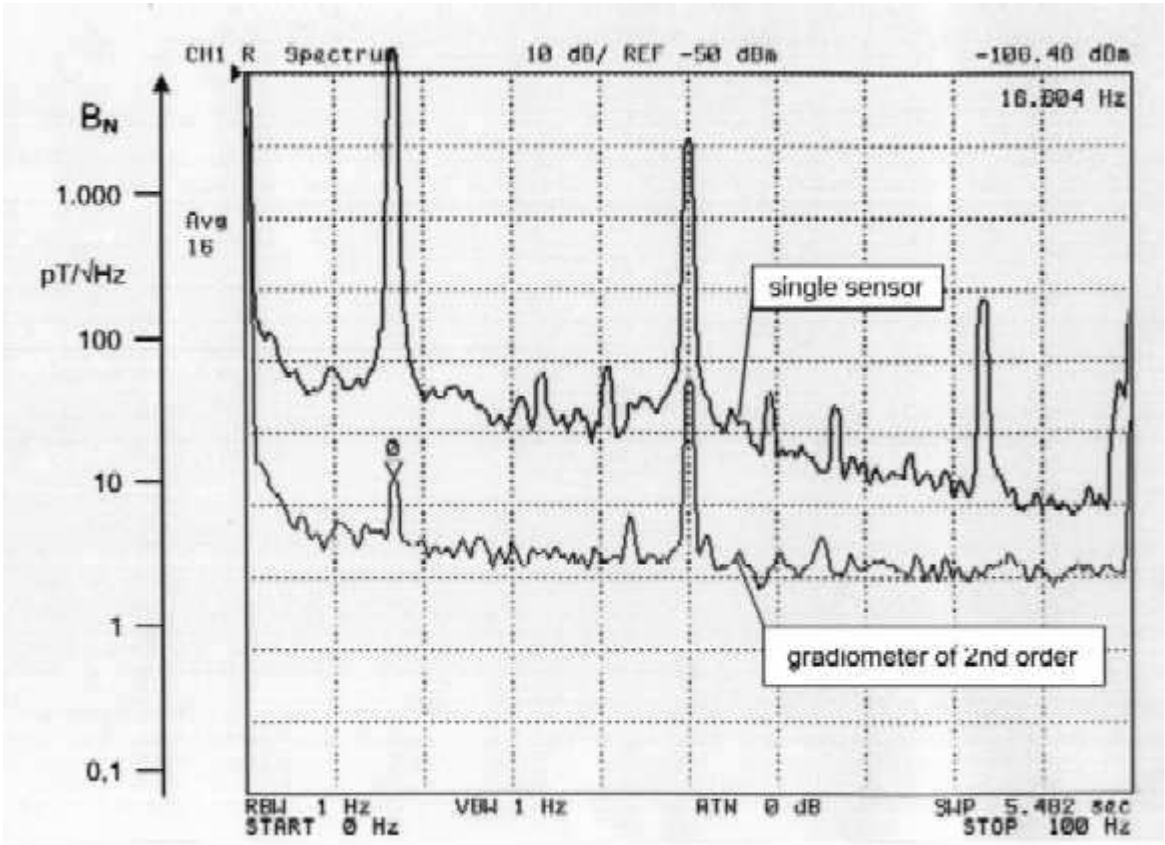

Figure 3: Noise Spectrum of Fluxgate Single Sensor and Gradiometer

Figure 3 shows the difference in the noise spectra of the lowest single sensor and the gradiometer. The comparison shows for example the reduction of a 16.33 Hz noise signal down to -60 dB. This

signal stems from an electrical train in a distance of about 200 m. The noise floor of the gradiometer is given by the noise of the single sensors and can not be further reduced by the gradiometer arrangement.
The premagnetisation of the device under test can be made either in tangential or in normal direction with respect to the device surface. The measurement system only detects the normal component of the magnetic field. Then a premagnetisation in normal direction will tend to give a monopole magnetic field distribution, while a premagnetisation in tangential direction will tend to give a dipole type distribution. If the inclusion is of rod shape it tends to result in a dipole type distribution if placed tangentially and to give a monopole distribution if placed normally.

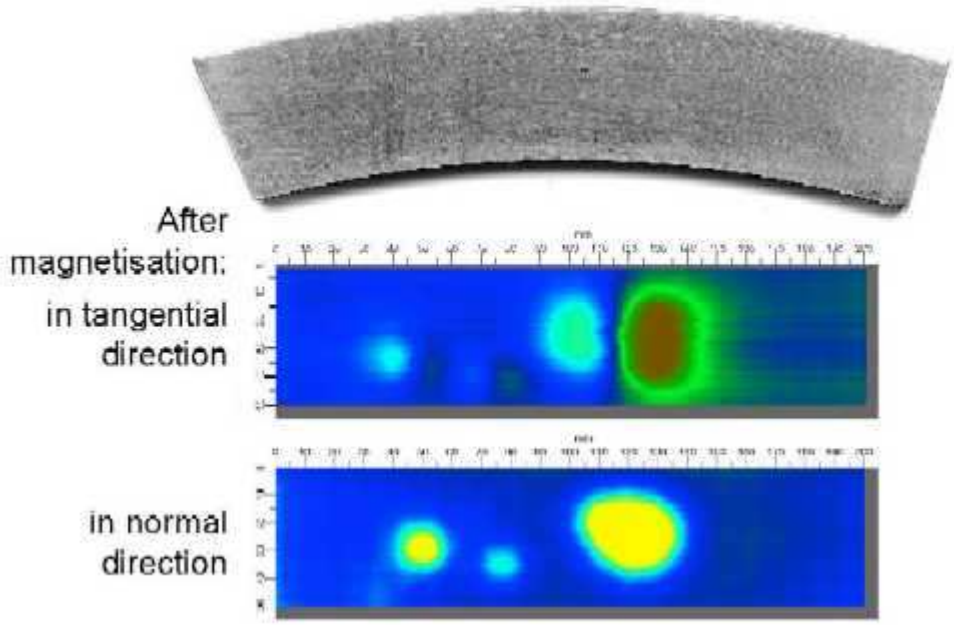

Figure 4: Photograph and MRM C-scans of sample 11a after tangential and normal premagnetisation

Figure 4 shows the influence of the direction of premagnetisation on an example of a Ti-6Al-4V sample with three tungsten carbide inclusions. Technical tungsten carbide for tool applications contains a small percentage of cobalt and therefore is slightly ferromagnetic. This is the reason why tungsten carbide inclusions can be detected by MRM.
For eddy current inspection small probes are used. Figure 5 presents four probes and their imaging properties.
The first row shows a gap probe that has to be scanned in touching mode over the surface. The image results from two drilled holes of 0.4 and 0.8 mm diameter and two eroded vertical slots of 0.4 and 0.8 mm length and 0.2 and 0.4 mm depth respectively in a flat titanium specimen. The second and the third row present cylinder core probes of absolute and differential type. The last row sketches a multi-differential probe providing more complicated images. For this paper the first and the second probes were used. More detailed information can be found in [4,5]. The working frequencies range from 600 kHz up to 4 MHz and drive the probes in single or multi-frequency mode depending on the task and the required penetration depth.

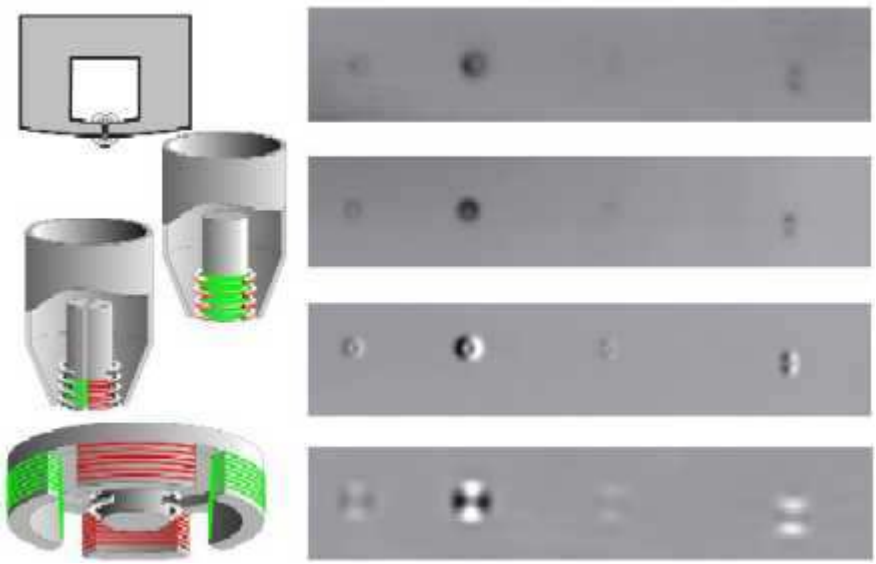

Figure 5: Eddy current probes and typical images

Figure 6 shows measurement results from sample 11a. The sample is made from Ti-6Al-4V and has sickle shape. It contains three splinters of a tungsten carbide tool as inclusions. Two inclusions are on the front surface and one big inclusion is on the back surface. The exact size of the inclusions is not known. Figure 6a shows the MRM C-scans from the front and from the back. It can be seen that the sample is transparent for this type of measurements. The inclusions can be seen with good signal to noise ratio from both sides.
The EC results are shown in Figure 6c. This method provides two images representing the real (EC-X) and the imaginary part (EC- Y) of the complex measurement signal. The geometric resolution of the probe is better than 0.3 mm. At the operating frequency of 3 MHz the lift-off signal was adjusted horizontally. Therefore small deformations of the surface caused by tool particles mostly generate horizontal signals (lift-off). On the other hand, embedded particles of tungsten carbide in the near surface region lead to mostly vertical signals due to their higher permeability. That is the basis for distinguishing both anomalies. The EC-Y image mirrors the particles as bright spots. The dark spots in the EC-X image represent local surface deformations.

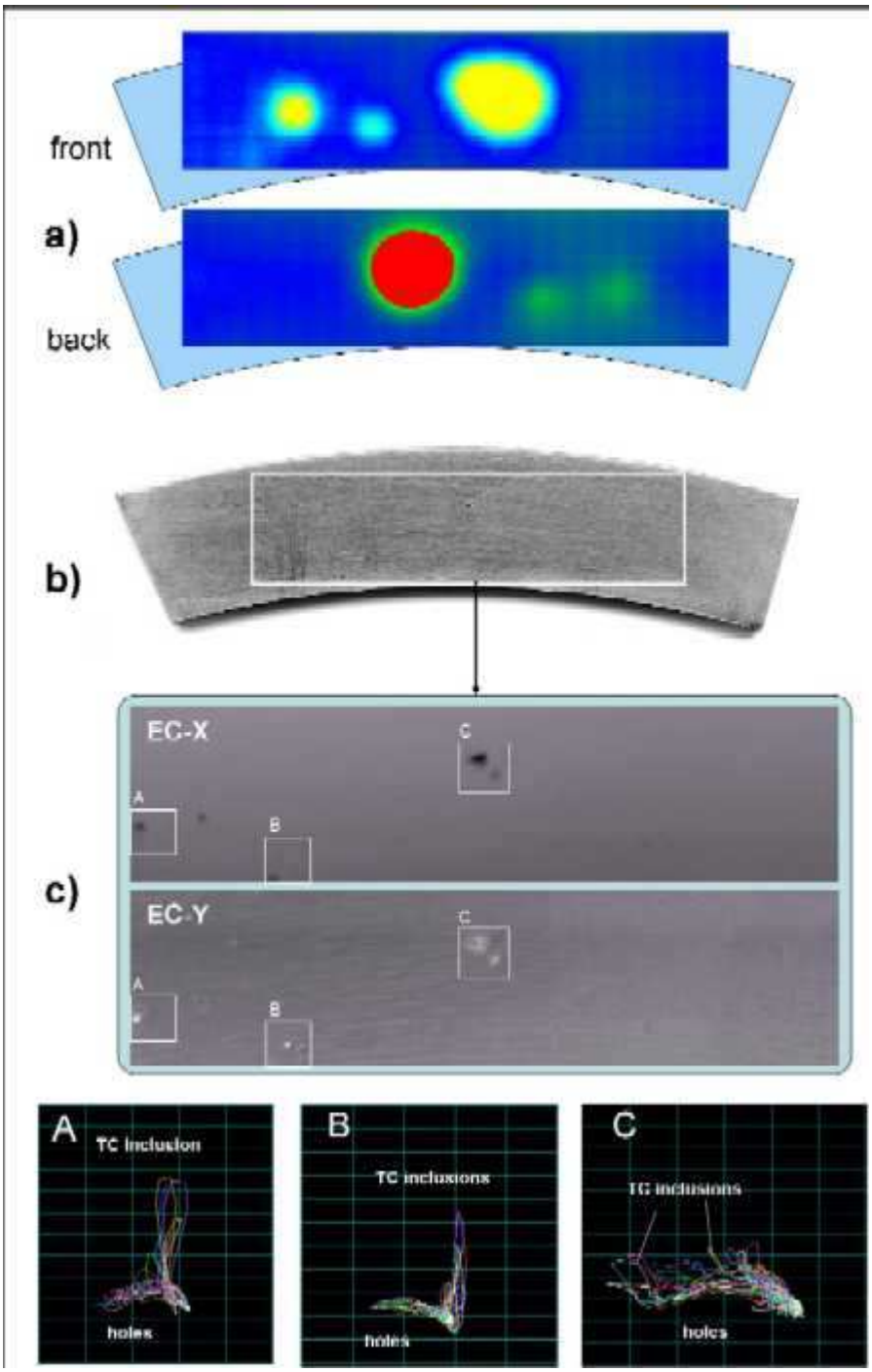

Figure 6: Sample 11a. a) MRM C-scan from front and from back, b) photograph, c) EC signals and analysis

Sample 11d is made from the same material and has a similar shape as sample 11c, see figure 7. The inclusions are also from technical tungsten carbide. They are produced by drilling well defined holes into the sample and pressing tungsten carbide material into these holes. Although the filling factors of the holes is not known the size of these inclusions is better defined than those in sample 11c. Table 1 gives details on the inclusions in sample 11d: there are 6 holes, 2 are empty and 4 are filled. The centre of figure 7 shows a photograph of sample 11d. On the top MRM C-scans are to be seen. The upper one of these two C-scans show results of scanning with the standard arrangement as described before, giving high amplitude sensitivity. The lower one of the two shows results from using an additional flux focusser which gives high spatial resolution with slightly reduced amplitude sensitivity. In a good display or printout all three inclusions on the left hand side can be seen as well as the big inclusion on the right hand side of sample 11d.

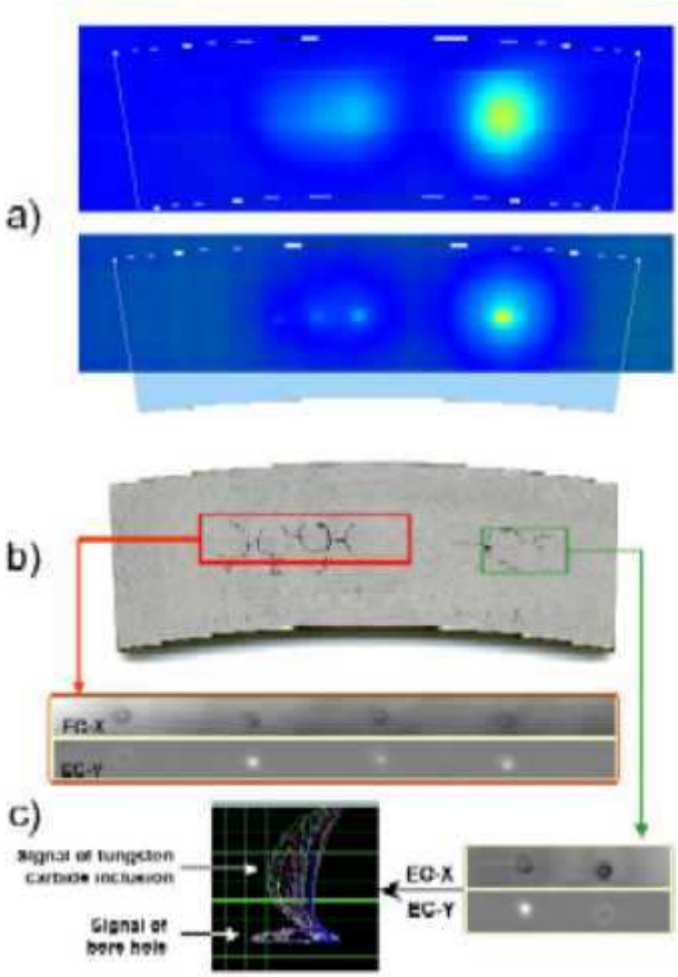

Figure 7: Sample 11d. a) MRM C-scan with high amplitude sensitivity and with high spatial resolution, b) photograph, c) EC signals

Table 1: Inclusions in sample 11d

Hole No.	Diameter of hole in mm	With/without WC inclusions
1	0,2	without
2	0,2	with
3	0,2	with
4	0,2	with
5	0,3	with
6	0,3	without

Eddy current inspection is able to detect and identify both the empty and the filled holes. The first scan was guided over the group of 0.3-mm-anomalies. A complex plane signal is given as an example showing the almost horizontal signal of the empty holes and the vertical signal of the tungsten carbide inclusions. The EC-Y image highlights the inclusion as a bright spot even describing its shape at the surface. The EC-X image contains the geometry information (edge effect) of the hole and the inclusion. The second scan covers the group of four 0.2-mm-holes. The images emphasize the superior resolution of this method. Running investigation is focused to quantify the detected anomalies.

Figure 8 shows a further MRM C-scan of two minute TC(Co) inclusions in Ti-6Al-4V. Their size is 0.07 mm x 0.05 mm diameter. They are oriented vertically with respect to the plane of the sample. The premagnetization was performed horizontally. Figure 8 shows that the detection results in dipole type magnetic field distributions with high signal-to-noise ratio. Taking into account the specific mass of TC it can be stated that the present state of the art of MRM allows the resolution of TC(Co) inclusions in the order of 1 microgram.

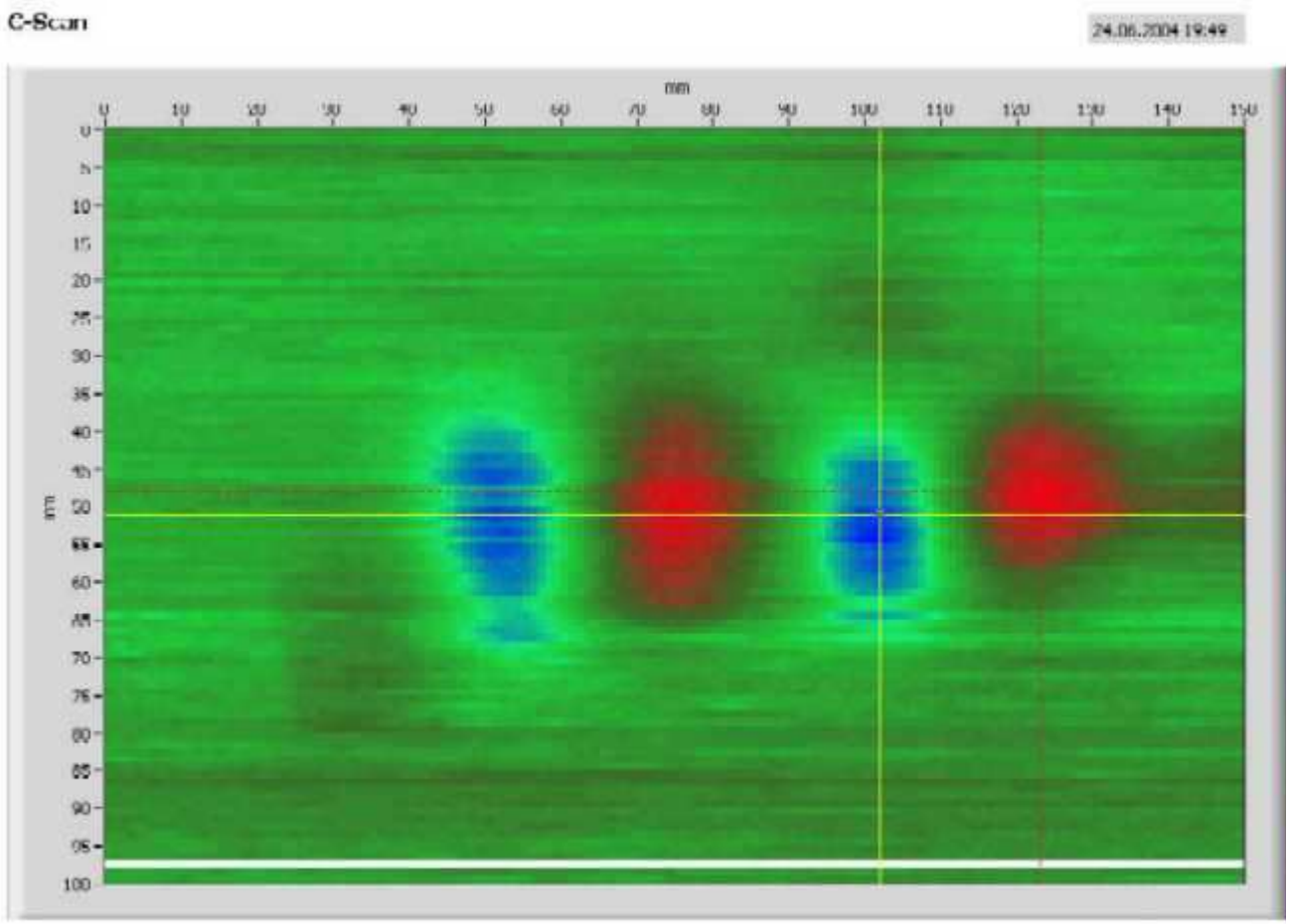

Figure 8: MRM C-scan of two TC(Co) inclusions of size 0.07 mm x 0.05 mm diameter

Using multi-frequency eddy current techniques a more detailed characterisation becomes possible. Figure 9 presents a large anomaly intentionally provoked by a breaking tool. The surface was heavily distorted and an inclusion remained at the ground of the deformation. The indicated area was scanned at three frequencies using an absolute probe. A multi-frequency algorithm was found to separate the permeability signal from the geometry. The multi-frequency (MF) visualisation lets recognize details of the shape and the orientation.

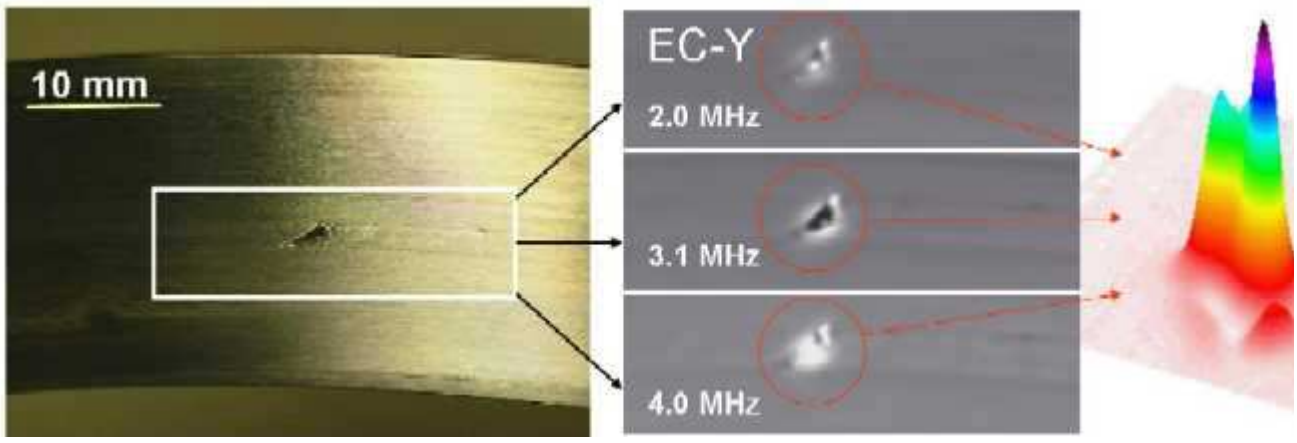

a) Photograph of the sample b) Images at different frequencies c) MF visualisation

Figure 9: Eddy current visualisation of a tungsten carbide inclusion in the titanium alloy Ti-6Al-4V.

3. Discussion

Both MRM and EC testing can be used to detect small ferromagnetic particles in a non-ferromagnetic surrounding. Both methods are complementary to each other in the following sense. For MRM the device under test is transparent, therefore also inclusions deep below the surface can be detected. EC testing has the advantage to give a higher spatial resolution.

4. Conclusions

The detection and characterisation of ferromagnetic inclusions in non-ferromagnetic alloys using the magnetic remanence method (MRM) and a special mode of eddy current (EC) testing was described. Both methods can detect extremely small inclusions. The advantage of MRM is the detectability of inclusions also deep below the surface. The advantage of EC testing is the higher spatial resolution.

The authors are extremely thankful to W.-D. Feist from MTU Aero Engines GmbH Munich for making the samples available to them.

References

[1] Y. Tavrin, M. Siegel, J. H. Hinken,: Standard Method for detection of magnetic defects in aircraft engine discs using a HTS SQUID gradiometer. IEEE Transactions on Applied Superconductivity, vol.9 (1999) no. 2, 3809-3812

[2] Verfahren zur Ermittlung von Defekten in Werkstuecken sowie Magnetfeldmessgeraet zur Durchfuehrung dieses Verfahrens. Patent DE 19746000C2, granted 16 May 2002

[3] H. Wrobel, Y. Tavrin, M. Wenk, J. H. Hinken: Fluxgate-Gradiometer für hochaufloesende Magnetometrie, ZfP-Zeitung, Ausgabe 88, Februar 2004, 41-43; see also http://www.elektrotechnik.hs-magdeburg.de/Mitarbeiter/hinken/news/n12.htm

[4] G. Mook, J. Simonin, R. Zielke, H.-A. Crostack, M. Maass: Testkoerper zur Einschaetzung des Aufloesungsvermoegens von Wirbelstromsystemen, Jahrestagung DGZfP 1999, Celle, BB 68/2, p. 751-760

[5] G. Mook, J. Pohl, F. Michel, T. Benziger, A. Hilbig: Non-Destructive Imaging Techniques for Damage Evaluation of Smart Materials. In: P.-J.. Winkler (ed.): Materials for Transportation